



Fast Fourier transform combined with phase leading compensator for respiratory motion compensation system

Chia-Chun Kuo^{1,2,3}, Ho-Chiao Chuang⁴, Ai-Ho Liao^{5,6}, Hsiao-Wei Yu⁷, Syue-Ru Cai⁴, Der-Chi Tien⁴, Shiu-Chen Jeng^{1,8}, Jeng-Fong Chiou^{1,7,9}

¹Department of Radiation Oncology, Taipei Medical University Hospital, Taipei, Taiwan; ²Department of Radiation Oncology, Wanfang Hospital, Taipei Medical University, Taipei, Taiwan; ³School of Health Care Administration, College of Management, Taipei Medical University, Taipei, Taiwan; ⁴Department of Mechanical Engineering, National Taipei University of Technology, Taipei, Taiwan; ⁵Graduate Institute of Biomedical Engineering, National Taiwan University of Science and Technology, Taipei, Taiwan; ⁶Department of Biomedical Engineering, National Defense Medical Center, Taipei, Taiwan; ⁷Taipei Cancer Center, ⁸School of Dentistry, College of Oral Medicine, ⁹Department of Radiology, School of Medicine, College of Medicine, Taipei Medical University, Taipei, Taiwan

Correspondence to: Prof. Ho-Chiao Chuang, Department of Mechanical Engineering, National Taipei University of Technology, No. 1, Sec. 3, Chung-Hsiao E. Rd., Taipei 10608, Taiwan. Email: hchuang@mail.ntut.edu.tw.

Background: The reduction of the delaying effect in the respiratory motion compensation system (RMCS) is still impossible to completely correct the respiratory waveform of the human body due to each patient has a unique respiratory rate. In order to further improve the effectiveness of radiation therapy, this study evaluates our previously developed RMCS and uses the fast Fourier transform (FFT) algorithm combined with the phase lead compensator (PLC) to further improve the compensation rate (CR) of different respiratory frequencies and patterns of patients.

Methods: In this study, an algorithm of FFT automatic frequency detection was developed by using LabVIEW software, using FFT combined with PLC and RMCS to compensate the system delay time. Respiratory motion compensation experiments were performed using pre-recorded respiratory signals of 25 patients. During the experiment, the respiratory motion simulation system (RMSS) was placed on the RMCS, and the pre-recorded patient breathing signals were sent to the RMCS by using our previously developed ultrasound image tracking algorithm (UITA). The tracking error of the RMCS is obtained by comparing the encoder signals of the RMSS and RMCS. The compensation effect is verified by root mean squared error (RMSE) and system CR.

Results: The experimental results show that the patient's respiratory patterns compensated by the RMCS after using the proposed FFT combined with PLC control method, the RMSE is between 1.50–5.71 and 3.15–8.31 mm in the right-left (RL) and superior-inferior (SI) directions, respectively. CR is between 72.86–93.25% and 62.3–83.81% in RL and SI, respectively.

Conclusions: This study used FFT combined with PLC control method to apply to RMCS, and used UITA for respiratory motion compensation. Under the automatic frequency detection, the best dominant frequency of the human respiratory waveform can be determined. In radiotherapy, it can be used to compensate the tumor movement caused by respiratory motion and reduce the radiation damage and side effects of normal tissues nearby the tumor.

Keywords: Fast Fourier transform (FFT); ultrasound image tracking; respiratory motion compensation

Submitted Aug 15, 2019. Accepted for publication Mar 16, 2020.

doi: 10.21037/qims.2020.03.19

View this article at: <http://dx.doi.org/10.21037/qims.2020.03.19>

Introduction

During the radiation therapy, the overall treatment can be affected due to patient's emotional stress. Therefore, the irregularity of the breathing signals might cause the base line shift of the organs in the body as well as the tumor, and thus, the radiation dose cannot be accurately delivered to the tumor (1). Respiratory movements also directly induce lung tumor shift, while the diaphragm that are highly correlated with lung tumor movement has a maximum displacement in superior-inferior (SI), right-left (RL), and anterior-posterior (AP) directions. The displacements are 50, 27.5, and 15 mm (2), respectively. Nowadays the most popular technology to improve the effectiveness of radiotherapy is real-time tracking and compensation, and typically combined with an imaging system for monitoring (3-5). Image-guided radiation therapy (IGRT) is an electronic digital image capturing system that combines a computerized tomography [cone beam CT (CBCT)] and X-ray [on-board imager (OBI)] on a linear accelerator (LINAC). The patient's CT image of the tumor can be obtained simultaneously by using IGRT, to correct the patient's body position and lock the precise range of tumor treatment at the earliest time (6). Due to many problems with the real-time tracking compensation system, it is impossible to compensate to the correct position immediately (7). In order to make the treatment better, many research teams have proposed different approaches to solve and improve the compensation effect.

Ichiji *et al.* (8) has reported a new prediction method of human respiration motion for accurate dynamic radiotherapy, so called the tumor tracking therapy. They proposed a time-variant seasonal autoregressive (TVSAR) model to further capture the time-variant and complex nature of various respiratory patterns. This model used the discrete Fourier transform (DFT) to perform the tumor tracking test of 105 tumor movements from the clinical database. The average tracking errors were 1.28 ± 0.87 and 1.75 ± 1.13 mm with 0.5 and 1.0 second predicted results, respectively. Prove that the methods they propose can outweigh the most advanced prediction methods. Kenneth *et al.* (9) indicated that the current clinically available electronic portal imaging device (EPID) has a frame rate limit of 7.5 Hz and the maximum frame rate is 30 Hz. They proposed an imaging signal filter to remove pulsing artifact on MV images, which consists of a wavelet decomposition followed by a fast Fourier transform (FFT). By using their proposed W-FFT filtering (wF), the pulsing artifact was

reduced. Their experimental results show that the Visicoil label at 0.05 cm results in a root mean square error (RMSE) >0.2 cm.

This study combines FFT with phase lead compensator (PLC) to develop a real-time automatic frequency detection algorithm. In 2007, Katsura *et al.* (10) have developed several vibration suppression control methods in order to solve vibration suppression and achieve robustness in motion control systems. However, in conventional vibration control systems, many studies have not considered the resonant frequency. They proposed a novel vibration control of a multimass resonant system based on PLC. It also clarifies the influence of the parameter variation of a disturbance observer on acceleration control system. In 2015, Golestan *et al.* (11) improved the filtering capability of the phase-locked loop (PLL) by incorporating the moving average filter (MAF) into its control loop. This method is at the cost of a slow transient response for the PLL, which is undesirable in most applications. However, adding a PLC to the MAF-PLL control loop can alleviate this problem. In 2018, Safaei *et al.* (12) discussed fractional-order phase-lead compensators to provide the required time domain definitions. They reported a simple analytical design technique, which is based on the minimization of pole-zero ratio subject to pole placement requirements. The necessary conditions of the pole's problem and the optimal parameters for the compensator are provided in their proposed method. Thus, a desired sensitivity can be provided by properly selecting the compensator's fractional-order in the acceptable range in order to have a robust compensator.

In 2015, our previous study (13) used the PLC to perform real-time tumor displacement tracking and compensation experiments, and we found that both ultrasound imaging system and respiratory motion compensation system (RMCS) have a serious system delay time problem. Although it has a good compensation effect on the sin wave input signals, when the PLC was used to compensate the human respiratory signals, the signal changes drastically and the compensation effect is not good (14). Therefore, in this study we used FFT algorithm combined with the existing PLC for respiratory motion compensation experiments, and cooperated with the Department of Radiation Oncology at the Taipei Medical University to conduct clinical trials. The diaphragm was used as a surrogate for the tumor tracking in the experiments. An ultrasound imaging system was used to observe the movement of the diaphragm and the real-time diaphragm motion signals were captured by using our

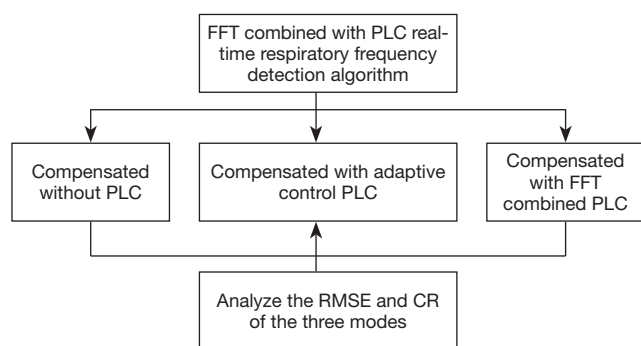


Figure 1 Experimental flow chart.



Figure 2 Diagram of clinical trial setup. (A) Ultrasound imaging system; (B) ultrasound probe.

previously developed ultrasound image tracking algorithm (UITA) (15). In the subsequent verification and respiration displacement compensation experiments, the ultrasound imaging system was used again to track the diaphragm phantom, to perform a real-time respiratory motion tracking and compensation experiments (16–21), because the diaphragm motion is highly related to the tumors near lung and liver.

The previously reported adaptive control algorithm (22) mainly calculates the average breathing time of the volunteer breathing signals, and establishes the gate

value to infer and determinate the generation of the next breathing cycle. The respiratory signal can be analyzed by the time reciprocal of the gate value to determine its dominant frequency. The breathing signal of the next cycle is estimated based on the calculated dominant frequency, but the setup of gate value is too low to correct the peak area of the breathing signal. The purpose of this study is to improve the real-time automatic respiratory frequency detection algorithm. Therefore, the FFT was used and combined with the PLC in this study to further improve the compensation effect of the breathing signal with dramatic changes.

Methods

Experimental method

This study proposes a real-time automatic frequency detection algorithm based on the FFT combined with PLC. The displacement compensation experiments of patient respiratory motion signals were performed in three modes, compensated without PLC, compensated with adaptive control PLC, compensated with FFT combined PLC. The RMSE and compensation rate (CR) are calculated to compare the difference among three modes in compensation performance. The experimental flow chart is shown in *Figure 1*.

Experimental equipment

The purpose of this study is to improve the automatic frequency detection method for the turning point (peak) of respiratory signal. The hardware devices used in clinical trials include ultrasound imaging system (Fukuda Denshi, UF-4000), Video Capture Card (CE310B, AverMedia). The software includes UITA (15), LabVIEW motion control software, and the clinical trial setup diagram is shown in *Figure 2*. The diaphragm movement of the patient's abdomen was observed through the ultrasound imaging system, and the diaphragm motion image was tracked and analyzed by UITA and then transmitting to LabVIEW. Hardware devices for compensation verification experiments include ultrasound imaging system (Fukuda Denshi, UF-4000), Video Capture Card (CE310B, AverMedia), RMCS, respiratory motion simulation system (RMSS), motion control card (National Instruments, PCI-7344). The composition of RMCS and RMSS includes an acrylic plate, a motor (Yaskawa, BA1SGM7A-04AFA61),

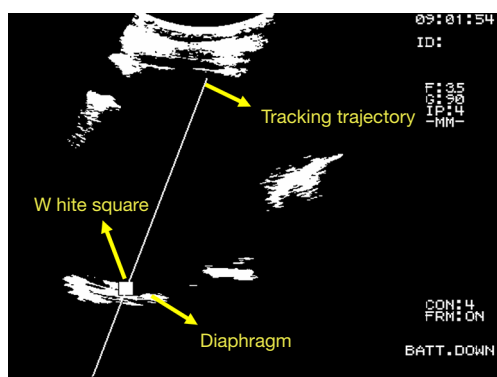


Figure 3 Ultrasound image analyzed by UITA. UITA, ultrasound image tracking algorithm.

a linear slide, and a ball screw. The software for the validation experiment included UITA, LabVIEW motion control software, and the phantom used in this study was a diaphragm phantom. The pre-recorded patient's diaphragm respiratory signal was input to the RMSS, and the diaphragmatic phantom movement on the RMSS was observed through the ultrasound imaging system. The ultrasound images of diaphragm motion were processed by the image binarization method via UITA, and the captured ultrasound image of diaphragm was presented at the brightest points. The phantom motion was tracked by a designed small white frame and the established tracking trajectory by the UITA. The diaphragm displacement was transmitted to the RMCS for compensation experiments. *Figure 3* shows an ultrasound image analyzed by UITA. The motors that drive the RMSS and RMCS and the encoder that records motors are both controlled by the LabVIEW control program and display the real-time position data of RMCS in the LabVIEW interface for easy operation.

Patient respiratory signals capturing

In this study, when measuring the respiratory signal of a patient, the clearest position of the diaphragm is measured on the ultrasound image and the tracking point is manually defined. Therefore, the initial diaphragm position of each patient on the ultrasound imaging is different. In order to verify the feasibility of using the proposed FFT combined with PLC in real-time automatic frequency detection algorithm for the compensation of patient's respiratory signals, breathing signals of 25 patients were used in this study (IRB 201902015) for verification experiments. The UITA with LabVIEW was used to capture the real-time

diaphragmatic motion signal of each patient, as shown in *Figure 4*. During the experiments, the ultrasound probe was placed on the patient's abdomen to observe the internal diaphragm movement, and the diaphragm motion of ultrasound images are instantly transmitted to the computer through the image capturing card. The diaphragm movement is then immediately tracked and analyzed through the UITA and the real-time diaphragm displacement signals were recorded by LabVIEW.

FFT

FFT is a linear integral transform for converting signals between the time domain and the frequency domain. There are many applications in physics and engineering. FFT is divided into several different forms, such as Fourier series, discrete-time Fourier transform, DFT, and Time-Frequency Analysis Transform. The formula of the FFT is as shown in Eq. [1].

$$F(\xi) = \int_{-\infty}^{\infty} f(x)e^{-2\pi i x \xi} dx \quad [1]$$

The variable x represents time (in seconds) and the conversion variable ξ represents frequency (in Hz).

The most common one is DFT, and the application includes FFT, spectrum analysis, data compression, partial differential equation, long integer, polynomial multiplication and orthogonal frequency-division multiplexing. Ichiji *et al.* (8) indicated that their developed TVSAR model uses the DFT. However, the main task in this study is to analyze the detected current respiratory signals and to calculate its dominant frequency for further respiratory signal detection and to infer the respiratory waveform of the next respiratory cycle. Therefore, there is no need to perform complex operations through the DFT, and the FFT can be used directly. In this study, the length of FFT is 10 seconds, the time resolution of respiratory signal is 0.01 second and the refresh ratio of the detected frequency is 0.1 Hz.

Instantaneous frequency automatic detection of FFT

According to the experimental results of the previous project, the important parameters a and k of the PLC (13) will change along with the frequency of the input respiratory signal, and we have also developed an automatic frequency detection system (22). It is mainly based on the adaptive control to instantly track and compensate for respiratory signals of different frequencies and waveforms. However, in order to make the RMCS system faster and more accurate

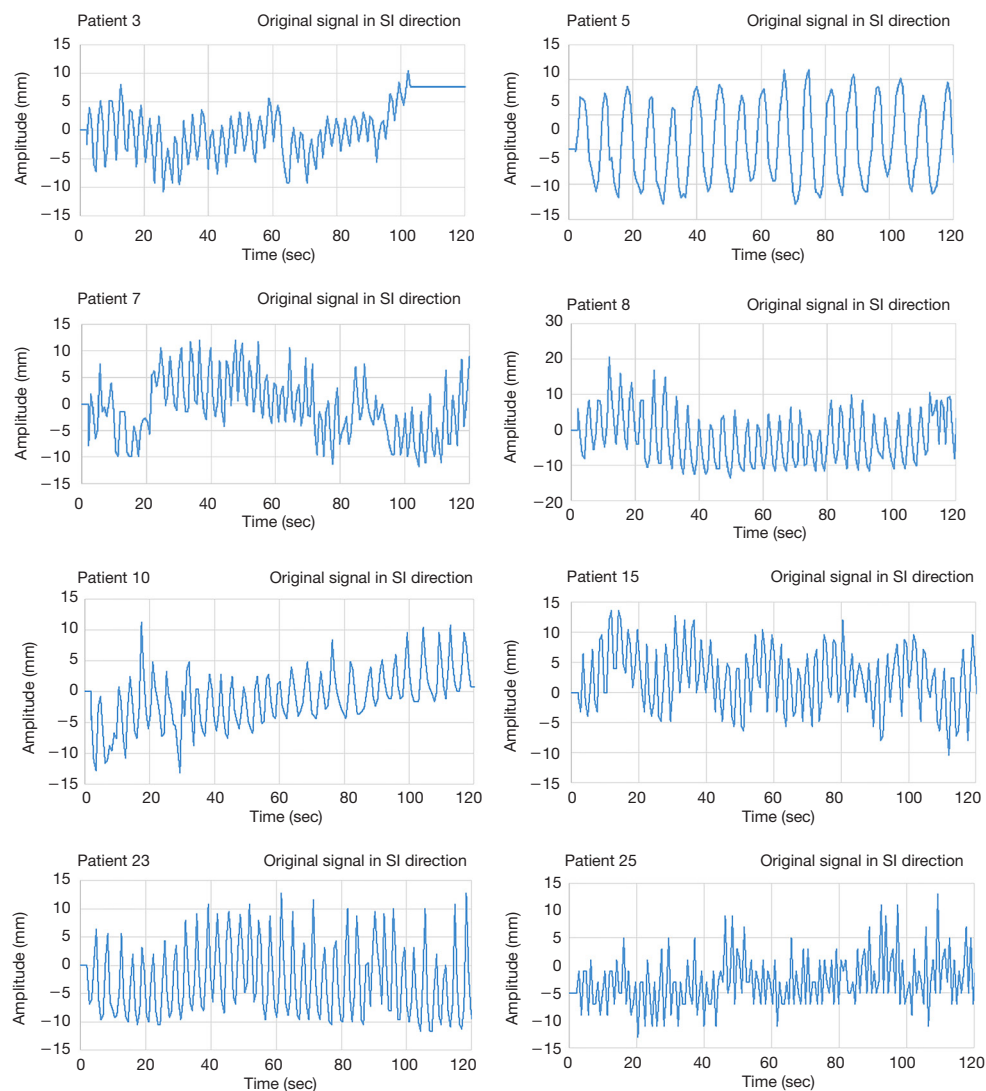


Figure 4 Captured diaphragmatic motion signals of eight patients.

in the case of non-lossy to improve the effectiveness of radiotherapy, this study developed a real-time automatic frequency detection module (algorithm) using FFT for the real-time analysis of the patient's respiratory signal. The signal analysis process was to filter the input respiratory signals in order to remove the noise, and converts the time domain signal into a frequency domain signal through the formula Eq. [1], and thus, calculates the average frequency over a period of time (5–10 seconds). Taking this as the target frequency value after the conversion, the respiratory waveform of the next cycle can be estimated by this target frequency value, and the program flow chart is shown in *Figure 5*.

Analysis of frequency domain

The FFT converts a time domain signal into a corresponding amplitude and phase at different frequencies. The frequency spectrum is the signal presentation of the time domain signal in the frequency domain, and the anti-FFT converts the spectrum back into the time domain signal. In this study, FFT was used to convert the respiratory signal of patients from the time domain into a frequency domain signal, and then the dominant frequency can be determined. Next, the LabVIEW control program obtains the PLC parameters according to the main frequency, and the PLC predicts the waveform of the respiratory signal of the next cycle. Moreover, it uses the

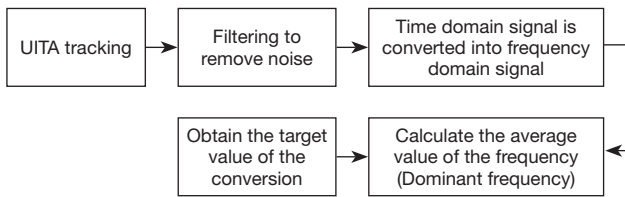


Figure 5 Flow chart of instant respiratory frequency signal automatic detection system.

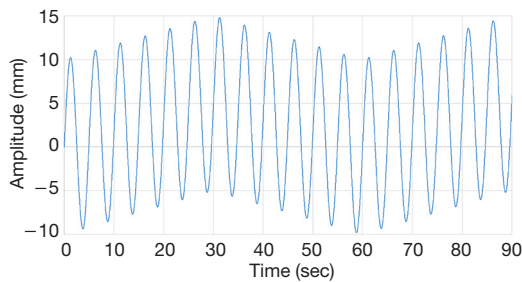


Figure 6 Selected original respiratory signal of the volunteers.

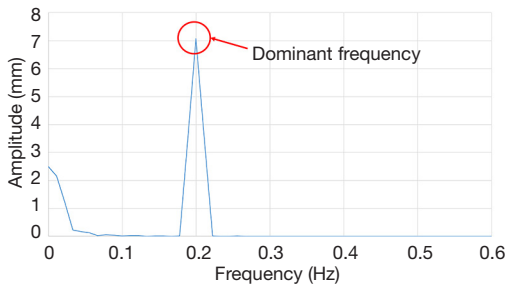


Figure 7 Frequency spectrum of the selected respiratory signal.

RMCS to perform a tracking compensation experiment on the respiratory signal. The respiratory signal waveform used in the compensation experiments, for example, the original respiratory waveform with a frequency of 0.2 Hz is shown in *Figure 6* and the frequency spectrum after the FFT signal processing is shown in *Figure 7*.

PLC

Our previously developed adaptive control PLC with RMCS could not completely correct the overall respiratory waveform during the respiratory motion compensation experiments (22), and caused the overall CR to decrease. Therefore, this study uses FFT combined with PLC to

correct the turning point (peak area) of respiratory signal, and it is expected to improve the CR, and the PLC formula used in the compensation experiments is shown as Eq. [2].

$$\left(\frac{s+1}{s+a}\right)k = \left(\frac{s}{s+a} + \frac{1}{s+a}\right)k \tag{2}$$

where ‘s + 1’ is the input to the compensator, ‘s + a’ is the output term, ‘s’ is the complex Laplace transform variable, ‘1’ is the zero frequency, ‘a’ is the pole frequency and ‘k’ is the gain factor. The value a is calculated through the dominant frequency, determined by the FFT, and the system delay time. After input value a into the control system, the phase of the respiratory signal can be advanced, which eliminates the delay time caused by the control system during signal transmission, calculation and analysis. However, this also changes the magnification of the input respiratory signals, causing the amplitudes of the input and output signals to be unequal, and thus, the gain coefficient k must also be added to compensate for the difference in amplitude.

Definition of RMCS tracking error

This study is expected to explore the CR before and after the target motion compensation. The target residual motion cannot be fully compensated due to the delay time of the RMCS. The tracking error of the target is calculated according to the instantaneous position signal of the motor encoder of the RMSS and RMCS. Moreover, the formula of the Root mean squared error (RMSE) for tracking error is shown as Eq. [3]. During the uncompensated state, since the RMCS is not activated, it is assumed that the value of *RMCS_i* at each time point is equal to 0 and the RMSE calculation is performed. The RMSE is defined as the difference in motor encoder position signals between RMSS and RMCS. The compensation performance is evaluated by CR, which is calculated by *RMSE_{compensated}* and *RMSE_{uncompensated}* as shown in Eq. [4]. The calculated RMSE between the adaptive control method with PLC and the proposed FFT combined with PLC will be discussed.

$$RMSE = \sqrt{\frac{\sum_{i=1}^n (RMSS_i - RMCS_i)^2}{n}} \tag{3}$$

$$CR(\%) = \left(1 - \frac{RMSE_{compensated}}{RMSE_{uncompensated}}\right) \times 100\% \tag{4}$$

Table 1 RMSE of patient's respiratory signals under three modes of compensation

Patient	Compensated without PLC, RMSE (mm)		Compensated with adaptive control PLC, RMSE (mm)		Compensated with FFT combined PLC, RMSE (mm)	
	RL	SI	RL	SI	RL	SI
P1	9.40	10.88	4.17	7.83	2.28	4.87
P2	9.81	10.85	7.05	10.20	4.20	6.68
P3	12.48	14.15	4.19	3.91	4.01	3.15
P4	14.76	12.62	3.29	9.24	3.50	6.57
P5	8.48	9.04	6.07	6.76	5.71	7.04
P6	10.54	14.27	4.48	10.25	4.33	8.31
P7	13.93	11.62	3.61	5.07	2.65	5.51
P8	8.55	10.03	5.60	3.68	3.40	7.63
P9	14.17	10.81	4.06	9.46	2.93	4.86
P10	13.33	10.71	2.07	5.38	2.30	4.62
P11	13.98	8.98	3.40	6.80	2.60	6.10
P12	12.52	9.37	3.46	7.91	2.17	4.56
P13	13.12	9.39	2.31	7.44	1.73	5.24
P14	11.47	8.56	2.85	6.41	1.50	3.23
P15	10.10	10.63	4.38	6.52	4.06	6.99
P16	12.10	8.88	3.80	5.34	3.03	3.87
P17	11.63	10.57	3.45	5.78	3.26	4.01
P18	8.52	12.68	3.71	8.87	2.23	7.23
P19	14.25	11.46	3.67	8.77	2.49	8.29
P20	9.33	8.72	2.72	5.32	3.16	4.51
P21	8.49	9.45	3.67	5.81	2.80	5.58
P22	11.99	10.45	3.52	6.20	2.59	5.61
P23	10.33	9.17	3.76	5.84	2.74	4.80
P24	9.86	8.92	5.75	5.27	3.47	4.24
P25	8.16	10.83	2.72	3.44	1.73	3.20

Pattern 1–25: patient respiratory signals. PLC, phase lead compensator; FFT, fast Fourier transform; SI, superior-inferior; RL, right-left; RMSE, root mean squared error.

Results

Comparison of RMSE under three modes compensation

In this experiment, the respiratory signals of 25 patients were input to the RMSS and then the RMCS was started. The respiratory motion compensation experiments were compared in three modes: compensated without PLC, compensated with adaptive control PLC, and compensated

with FFT combined PLC. The calculated RMSE under three modes in SI and RL directions is shown in *Table 1*. The RMSE without PLC compensation has average values of 11.25 and 10.52 mm in RL and SI directions, respectively, and the RMSE with adaptive control PLC compensation has average values of 3.91 and 6.7 mm in RL and SI directions, respectively. The RMSE using FFT combined with PLC compensation has an average of 2.99

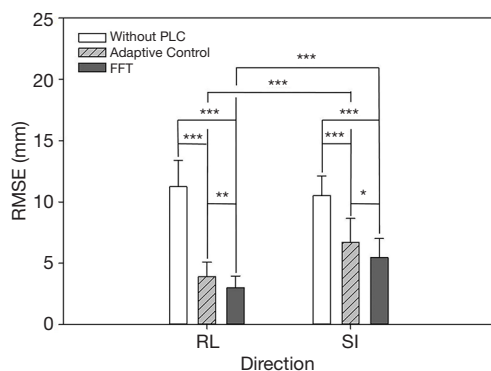


Figure 8 Comparison of the average RMSE among three modes in the RL and SI directions (* means a significant difference $P < 0.05$; ** means a significant difference $P < 0.01$; *** means a significant difference $P < 0.001$). RMSE, root mean squared error; RL, right-left; SI, superior-inferior.

and 5.47 mm in RL and SI directions, respectively. It can be found that the tracking error has a significant drop by using a PLC, and the compensation effect with using the FFT combined with PLC is the best. In addition, the average RMSE in the RL and SI directions among three modes were also compared, and the P value test was used to determine that the results of the comparison between the three modes were significantly different ($P < 0.001$). The comparison between the adaptive control PLC compensation and the FFT combined with PLC compensation in the RL and SI directions are ($P < 0.01$) and ($P < 0.05$), respectively as shown in *Figure 8*.

Comparison of CR under three modes compensation

In addition to comparing the calculated RMSE under three compensation modes, this study also compares the results of the CR and determines the difference in compensation effectiveness between the adaptive control PLC and the FFT combined with the PLC as shown in *Table 2*. It indicates that the CR without PLC compensation are between 1.59–57.24% and 7.56–56.89% with average values of 35.58% and 42.73% in RL and SI directions, respectively. CR with adaptive control PLC compensation is between 68.51–88.94% and 42.78–83.51%, with average values of 80.68% and 65.89% in RL and SI directions, respectively. The CR using FFT combined with PLC compensation is between 72.86–93.25% and 62.3–83.81%, and the average value is 84.93% and 72.34% in RL and SI directions, respectively. In *Table 2*, the CR value of using FFT

combined with PLC is the best. In addition, the average CR in the RL and SI directions among three modes were also compared, and the P value test was used to determine that the results of the comparison between the three modes were significantly different ($P < 0.001$). The comparison between the adaptive control PLC compensation and the FFT combined with PLC compensation in the RL and SI directions are ($P < 0.01$) and ($P < 0.05$), respectively as shown in *Figure 9*.

Comparison of the tracking effectiveness between adaptive control with PLC and FFT combined with PLC under patient's respiratory signals

In this experiment, three modes of control methods were used to perform the respiratory waveform compensation experiments to compare the RMSE and CR, and then the difference between the adaptive control PLC and the FFT combined with the PLC modes under the patient's respiratory signal was further discussed, as shown in *Figure 10*. In *Figure 10*, whether it is in RL or SI directions, the respiratory waveform in patient 1 was to use the adaptive control PLC (green) to track the original respiratory waveform (red), and the tracking result is that the green waveform is off-center axis, resulting in a waveform (green) goes above from the red line. Using the proposed algorithm, FFT combined with the PLC (blue), the tracking results are trackable to the turning point (peak area) of the partial respiratory waveform (red). The respiratory waveform of patient 9 uses the adaptive control PLC (green) method, and the result is that the turning point (peak area) of the respiratory waveform (red) is not tracked. Therefore, it shows that by using the FFT combined with PLC (blue), it has a significant tracking performance at the turning point (peak area) of the respiratory waveform. In addition, the Patient 14 uses the method of adaptive control PLC (green) and the results show that the turning point (peak area) of the respiratory waveform cannot be completely tracked. However, if the FFT combined with the PLC (blue) control method was used, the results indicated that the partial turning point of the respiratory waveform was tracked.

Discussion

In this study, the proposed FFT combined with PLC control method and the RMCS were both used for respiratory motion compensations. The RMSE value was calculated in both RL and SI directions from the

Table 2 CR of patient's respiratory signals under three modes of compensation

Patient	Compensated without PLC, CR (%)		Compensated with adaptive control PLC, CR (%)		Compensated with FFT combined PLC, CR (%)	
	RL	SI	RL	SI	RL	SI
P1	52.25	40.25	78.81	61.53	88.73	73.4
P2	53.97	40.83	69.23	48.56	78.6	66.12
P3	24.56	8.6	77.53	80.42	79.07	83.81
P4	8.32	23.57	83.1	52.56	83.47	67.05
P5	57.24	54.31	68.51	65.34	72.86	64.1
P6	45.69	7.56	75.89	42.78	77.82	56.82
P7	18.95	32.85	82.72	73.88	86.59	72.8
P8	56.31	49.02	71.58	83.51	82.53	62.3
P9	1.59	41.05	79.52	52.66	85.7	75.43
P10	12.95	41.28	88.94	72.41	88.6	76.14
P11	18.99	55.71	82.05	65.84	86.78	68.9
P12	25.02	52.4	81.53	60.48	89.52	76.57
P13	11.32	52.67	86.12	62.35	92.57	73.6
P14	34.67	56.89	85.78	66.12	93.25	83.64
P15	48.5	43.52	77.44	65.38	79.2	65.03
P16	28.4	55.13	84.53	72.68	84.6	80.47
P17	36.41	42.85	83.53	71.59	82.9	79.1
P18	52.86	22.46	82.09	54.94	88.97	63.33
P19	3.75	35.49	82.42	55.28	84.5	56.37
P20	51.86	56.03	86.46	72.79	83.71	77.08
P21	56.18	51.28	85.73	71.48	86.12	74.2
P22	38.91	44.53	83.22	66.5	86.73	74.01
P23	42.59	53.47	81.23	71.9	85.3	75.8
P24	53.13	55.31	72.63	73.69	82.57	78.65
P25	55.07	50.48	86.37	82.46	92.57	83.72

Pattern 1–25: patient respiratory signals. PLC, phase lead compensator; FFT, fast Fourier transform; SI, superior-inferior; RL, right-left; CR, compensation rate.

patient's respiratory signals, and then compared with other research teams. In this study, the experimental results show that the average RMSE is 5.47 and 2.99 mm in SI and RL directions, respectively. Lee *et al.* (23) reported a Couch-based tracking system based on respiratory data and tracked the respiratory signal using a 3D camera of the AlignRT system. Their experimental results show that the maximum RMSE is 7.54 mm under load. The

accuracy and repeatability of the Z direction in the patient data is very poor, and the RMSE of the added load in all directions is within 1.0 mm. D'Souza and McAvooy (24) used a Hexapod™ treatment bed for respiratory motion compensation experiments and proposed an internal model controller to simulate the feedback control of respiration-induced target motion. Their experimental results show that under input the step signal, the RMSE is below 3 mm.

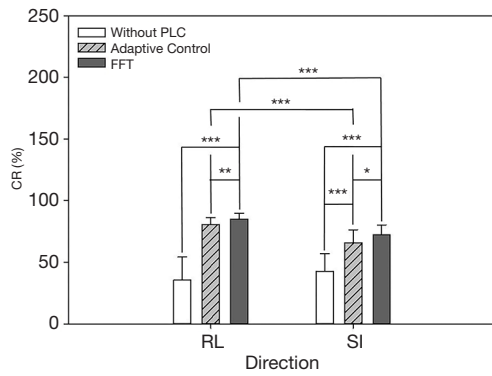


Figure 9 Comparison of the average CR among three modes in the RL and SI directions (* means a significant difference $P < 0.05$; ** means a significant difference $P < 0.01$; *** means a significant difference $P < 0.001$). CR, compensation rate; RL, right-left; SI, superior-inferior.

Although the results of their experiments are not much different from this study, the input signal they used is a step signal, which is quite different from the human respiratory signals. Their results obtained from 12 patients using skin markers placed on the patient’s abdomen. In addition, when simulating a faster treatment bed, the residual motion (uncompensated displacement) under feedback control is typically < 0.3 cm. Haas *et al.* (25) developed a patient support system (PSS) to fix tumors under radiation during radiotherapy and tracked the target with a digital camera. They also used an experimental and clinical Elekta precise table (TM) for validation tests. Their results show that the obtained maximum RMSE in the RL and SI directions after compensation is 5.21 and 4.46 mm, respectively. In this study, our tracking method is to use ultrasound images to observe the real-time internal diaphragm motion, which

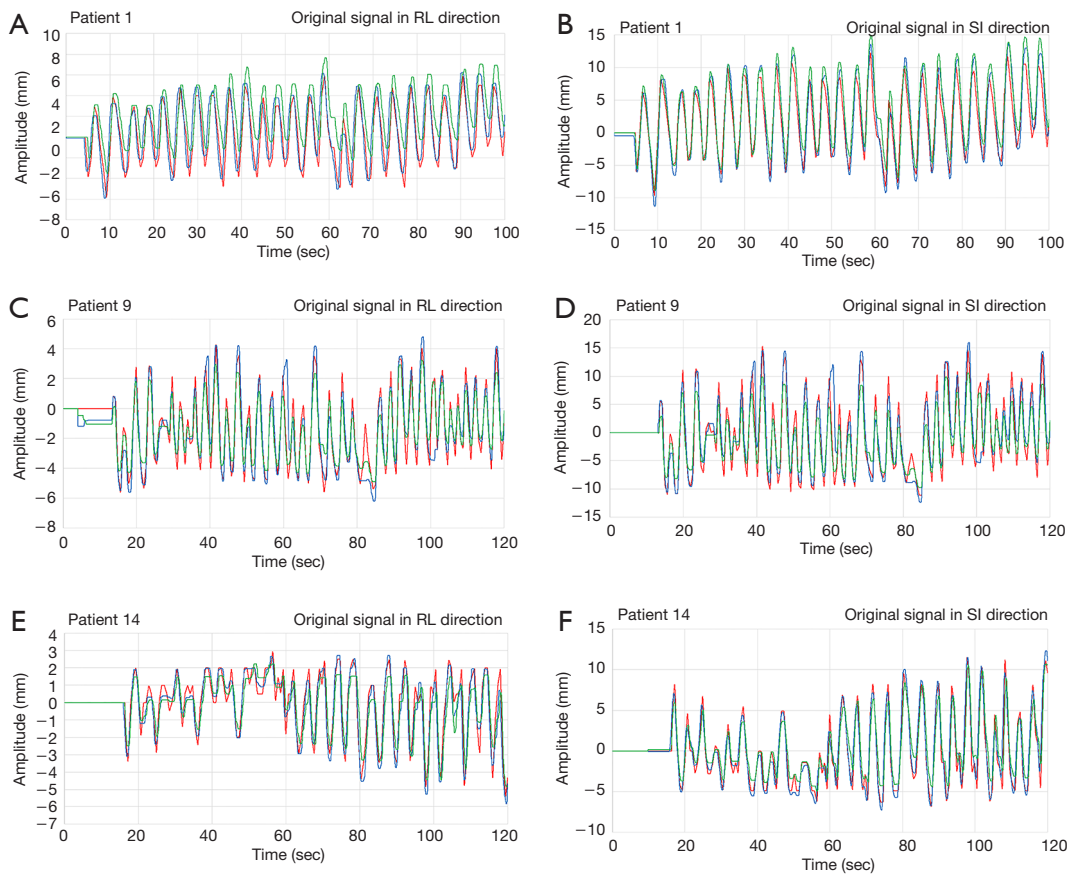


Figure 10 Comparison chart of adaptive control with PLC and FFT combined with PLC in the patient respiratory signals. The red waveform is the patient original respiration signal, the green waveform is the tracking compensation signal by adaptive control with PLC, and the blue waveform is the tracking compensation signal by using FFT combined with the PLC. (A), (C), and (E) are in RL direction, and (B), (D), and (F) are in SI direction. (A), (B): patient 1; (C), (D): patient 9; (E), (F): patient 14. PLC, phase lead compensator; FFT, fast Fourier transform; RL, right-left; SI, superior-inferior.

is highly correlated with lung tumors. It is more capable of presenting the true movement pattern of organ tissues *in vivo* than the *in vitro* tracking methods of other research teams.

The results of the experiment show that the obtained RMSE of using the FFT combined with PLC has significantly improved in RL direction. However, several patients respiratory motion waveform is worse than using the adaptive control PLC (patient 5, 7, 8, and 15) in SI direction, mainly because the patient's respiratory waveform changes more severely than healthy volunteers, and their frequency changes quickly. Among them, the respiratory motion waveform of patient 7 may not be able to track to the original respiratory waveform due to the large amplitude changes even using the proposed FFT combined with PLC control method. Although the respiratory waveform of Patient 8 does not have a large fluctuation in the amplitude of the respiratory waveform, the amplitude change during 10–20 seconds is more severe, the respiratory frequency is also more rapid, and the compensation effect in SI direction is relatively worse than that of using adaptive control PLC method. The results also show that by using the adaptive control PLC, it has a better compensation effect on those respiratory waveforms with relatively small amplitude. The amplitude of the respiratory waveform of patient 15 is more severe than that of patient 7, and there is also a baseline shift when the respiratory frequency is very fast. Therefore, the compensation effect of both FFT combined with PLC and adaptive control PLC control methods in SI direction is obviously worse than in RL direction.

It can be seen from the CR value that the compensation effect of using FFT combined with PLC is better than the other two modes, but the obtained data also reveals that the CR values between FFT combined with PLC and adaptive control PLC are very close in either RL or SI directions of some patients. For example, in the respiratory waveform of patient 15, the results of the compensation effect in two control methods are similar. However, most of the compensation effects in RL direction are higher than in SI direction, mainly because the amplitude of respiratory waveforms of patients in RL direction is much smaller than that of SI direction, which is related to the respiratory motion signals of patients in clinical trials. Because the internal organs are very close to the diaphragm or the patient's body is very tired, it will indirectly or directly affect the observation of ultrasound images. The respiratory motion waveform of each patient in the

RL direction will be disturbed by the above conditions. Furthermore, the amount of change in the respiratory displacement in RL direction is less than that of the SI direction. The experimental results show that the CR of the FFT combined with the PLC control method in SI and RL direction are 83.81% and 93.25%, respectively.

From the results mentioned above, the tracking results indicate that the tracking effect of using FFT combined with PLC is better than that of the adaptive control PLC. Because the FFT used in this study can convert the respiratory signal into a frequency domain signal, the dominant frequency can be directly obtained, which is used to predict the respiratory waveform of the next cycle in the dominant frequency of the respiratory signal. However, both the adaptive control PLC and the FFT combined with the PLC have a poor performance in tracking the turning point (peak area) of the very small amplitude (<3 mm) of the respiratory waveform. For example, the respiratory waveform of patient 14 has some peaks or valleys that are extremely small displacements. Compensation using RMCS will have poor compensation results, because the DC motor used in RMCS is one of the reasons. The RMSS uses a servo motor. The encoder of the DC motor has an error and the sensitivity is not as high as the servo motor. If a servo motor is used, the compensation effect will be better than a DC motor, especially for the respiratory waveforms with very small amplitudes. However, this kind of respiratory waveform is only a small part. For most respiratory waveforms with amplitudes of 5–15 mm, the DC motor used in the RMCS still has food compensation results. For example, after using the FFT combined with PLC, the CR of the respiratory waveform of patient 1 in RL direction is up to 88.73%. Moreover, from the comparison results of the P value test, the FFT combined with the PLC compensation was significantly different in both RL and SI directions in the RMSE and CR ($P < 0.001$).

In this study, the patient's comfort was considered in clinical human trials. We found out that the clamping of the ultrasound probe through the clamp overstressed the patient's abdomen. Therefore, the patient may feel uncomfortable and the body movement may cause the ultrasound probe to shift off the abdomen and become unusable. Therefore, in our clinical trials hand-held ultrasound probes was performed to capture diaphragm motion signals. In addition, after verification experiments, it was found that the difference between the respiratory motion waveform of patients and the respiratory motion

waveform of normal volunteers is that the analyzed value of imaging binary method used by UITA mostly is within the range of 180–220 for normal volunteers, and the patient's value is 70–120. Therefore, the ultrasound image after UITA processing in addition to the diaphragm also has other noise, for example: water, organs, flatulence.

This study used the ultrasound image tracking system to track real-time diaphragm movement as a surrogate to replace tumor movement. Even though the diaphragm is highly correlated with the respiratory displacement of lung and liver tumors, their amplitude is not exactly the same. In clinical trials, it is difficult to obtain the diaphragm motion signal of the patient, because the hospital usually performs the treatment plan first, and then carries out the clinical experiments that might increase the extra physical load on the patients. Therefore, the during of using ultrasound images to observe the patient's diaphragm movement will be reduced, and the length of the ultrasound imaging signal will be shortened, averaging 2–3 minutes. Even the presence of other organs or fluids around the diaphragm can affect the observation of ultrasound images. In this study, the proposed FFT combined with PLC control method was used to perform respiratory signal compensation experiments on patients with irregular respiratory motion waveforms. The experimental results showed that the FFT combined with PLC method significantly improved the turning point of respiratory signals, which is better than that of using adaptive control PLC method. However, if the used ultrasound imaging system is not good enough, the recorded respiratory motion waveform will be disturbed by other organs in the body. Therefore, if an ultrasound probe with a better depth of penetration is used in the future, it could make the ultrasound image quality better and more clearly observe the diaphragm movement so that the binary imaging value will also be increased by UITA, and the ultrasound imaging of the diaphragm motion will be less susceptible to interference from surrounding organs.

Conclusions

This study proposes a new method of using FFT combined with PLC applied to RMCS and UITA for real-time respiratory motion tracking compensation, and compares the difference in CR between FFT combined with PLC and adaptive control PLC. The experimental results show that the CR of FFT combined with PLC method in SI and RL to respiratory signals are 83.81% and 93.25%, respectively. In addition, this study also performed the P value test to

determine the difference of different compensation methods and the results show that the FFT combined with PLC compensation and adaptive control PLC compensation is significant difference in both RL direction and SI directions, indicating the compensation effect of using FFT combined with PLC control method is better. In this study, ultrasound images are used to track the real-time target motion and combined with UITA to calculate the displacement of the target. This tracking method is non-invasive, non-radiative, and can monitor the real-time organs movement in the body, and then compensate for respiratory motion with RMCS. Furthermore, during the radiotherapy the tumor movement induced by respiratory exercise can be improved, and the radiation damage and side effects of normal tissues surrounding the tumor are reduced.

Acknowledgments

The authors would like to express their appreciation to the Taipei Medical University Hospital, Taiwan for providing the financial and facilities support for this study.

Funding: This work was supported by the National Taipei University of Technology and Taipei Medical University Hospital under Contract USTP-NTUT-TMU-108-03.

Footnote

Conflicts of Interest: All authors have completed the ICMJE uniform disclosure form (available at <http://dx.doi.org/10.21037/qims.2020.03.19>). The authors have no conflicts of interest to declare.

Ethical Statement: All procedures performed in studies involving human participants were in accordance with the ethical standards of the institutional and/or national research committee and with the 1964 Helsinki Declaration and its later amendments or comparable ethical standards. Informed consent was obtained from all individual participants included in the study. The ethical approval is approved by the Taipei Medical University Hospital under the reference number: IRB 201902015.

Open Access Statement: This is an Open Access article distributed in accordance with the Creative Commons Attribution-NonCommercial-NoDerivs 4.0 International License (CC BY-NC-ND 4.0), which permits the non-commercial replication and distribution of the article with the strict proviso that no changes or edits are made and the

original work is properly cited (including links to both the formal publication through the relevant DOI and the license). See: <https://creativecommons.org/licenses/by-nc-nd/4.0/>.

References

- Li Y, Ma J, Chen X, Tang F, Zhang X. 4DCT and CBCT based PTV margin in Stereotactic Body Radiotherapy(SBRT) of non-small cell lung tumor adhered to chest wall or diaphragm. *Radiat Oncol* 2016;11:152.
- Wysocka B, Kassam Z, Lockwood G, Brierley J, Dawson LA, Buckley CA, Jaffray D, Cummings B, Kim J, Wong R, Ringash J. Interfraction and Respiratory Organ Motion During Conformal Radiotherapy in Gastric Cancer. *Int J Radiat Oncol Biol Phys* 2010;77:53-9.
- Wilbert J, Baier K, Hermann C, Flentje M, Guckenberger M. Accuracy of Real-time Couch Tracking During 3-dimensional Conformal Radiation Therapy, Intensity Modulated Radiation Therapy, and Volumetric Modulated Arc Therapy for Prostate Cancer. *Int J Radiat Oncol Biol Phys* 2013;85:237-42.
- Hansen R, Ravkilde T, Worm ES, Toftegaard J, Grau C, Macek K, Poulsen PR. Electromagnetic guided couch and multileaf collimator tracking on a TrueBeam accelerator. *Med Phys* 2016;43:2387-98.
- Lang S, Zeimet J, Ochsner G, Schmid Daners M, Riesterer O, Klöck S. Development and evaluation of a prototype tracking system using the treatment couch. *Med Phys* 2014;41:021720.
- Image guided radiation therapy (IGRT) - Arun Puranik, MD. Available online: <http://igrt.com/>
- Fast MF, O'Shea T, Nill S, Oelfke U, Harris E. First evaluation of the feasibility of MLC tracking using ultrasound motion estimation. *Med Phys* 2016;43:4628-33.
- Ichiji K, Homma N, Sakai M, Takai Y, Narita Y, Abe M, Sugita N, Yoshizawa M. Respiratory motion prediction for tumor following radiotherapy by using time-variant seasonal autoregressive techniques. *Proc Annu Int Conf IEEE Eng Med Biol Soc (EMBS)* 2012;2012:6028-31.
- Kenneth P, Dirk V, Iwein Van de V, Rafik El M, Tom D, Mark De R. Fiducial marker and marker-less soft-tissue detection using fast MV fluoroscopy on a new generation EPID: Investigating the influence of pulsing artifacts and artifact suppression techniques. *Med Phys* 2019;41:101911.
- Katsura S, Ohnishi K. Absolute Stabilization of Multimass Resonant System by Phase-Lead Compensator Based on Disturbance Observer. *IEEE Transactions on Industrial Electronics* 2007;54:3389-96.
- Golestan S, Guerrero JM, Abusorrah AM. MAF-PLL With Phase-Lead Compensator. *IEEE Transactions on Industrial Electronics* 2015;62:3691-5.
- Safaei M, Tavakoli S. Tuning of robust fractional-order phase-lead compensators using pole placement and pole-zero ratio minimization. *Journal of Vibration and Control* 2018;24:5379-90.
- Chuang HC, Hsu H, Nieh S, Tien D. The feasibility of the auto tuning respiratory compensation system with ultrasonic image tracking technique. *J Xray Sci Technol* 2015;23:503-16.
- Ting LL, Chuang H, Kuo C, Jian L, Huang M, Liao A, Tien D, Jeng S, Chiou J. Tracking and compensation of respiration pattern by an automatic compensation system. *Med Phys* 2017;44:2077-95.
- Kuo CC, Chuang HC, Teng KT, Hsu HY, Tien DC, Wu CJ, Jeng SC, Chiou JF. An autotuning respiration compensation system based on ultrasound image tracking. *J Xray Sci Technol* 2016;24:875-92.
- Boussuges A, Gole Y, Blanc P. Diaphragmatic Motion Studied by M-Mode Ultrasonography. *Chest* 2009;135:391-400.
- Haji K, Royse A, Tharmaraj D, Haji D, Botha J, Royse C. Diaphragmatic regional displacement assessed by ultrasound and correlated to subphrenic organ movement in the critically ill patients—an observational study. *J Crit Care* 2015;30:439.e7-439.e13.
- Ting LL, Chuang H, Liao A, Kuo C, Yu H, Zhou Y, Tien D, Jeng S, Chiou J. Experimental verification of a two-dimensional respiratory motion compensation system with ultrasound tracking technique in radiation therapy. *Phys Med* 2018;49:11-8.
- Zhang Y, Folkert MR, Huang X, Ren L, Meyer J, Tehrani JN, Reynolds R, Wang J. Enhancing liver tumor localization accuracy by prior-knowledge-guided motion modeling and a biomechanical model. *Quant Imaging Med Surg* 2019;9:1337-49.
- Dietrich CF, Teufel A, Sirlin CB, Dong Y. Surveillance of hepatocellular carcinoma by medical imaging. *Quant Imaging Med Surg* 2019;9:1904-10.
- Yan F, Song Z, Du M, Klibanov AL. Ultrasound molecular imaging for differentiation of benign and malignant tumors in patients. *Quant Imaging Med Surg* 2018;8:1078-83.
- Kuo CC, Chuang H, Yu H, Huang J, Tien D, Jeng S, Chiou J. Adaptive control of phase leading compensator parameters applied to respiratory motion compensation

- system. *J Xray Sci Technol* 2019;27:715-29.
23. Lee S, Chang K, Shim J, Cao Y, Lee C, Cho S, Yang D, Park Y, Yoon W, Kim C. Evaluation of mechanical accuracy for couch-based tracking system (CBTS). *J Appl Clin Med Phys* 2012;13:3818.
 24. D'Souza WD, McAvoy T. An analysis of the treatment couch and control system dynamics for respiration-induced motion compensation. *Med Phys* 2006;33:4701-9.
 25. Haas OC, Skworcow P, Paluszczyszyn D, Sahih A, Ruta M, Mills J. Couch-based motion compensation: modelling, simulation and real-time experiments. *Phys Med Biol* 2012;57:5787-807.

Cite this article as: Kuo CC, Chuang HC, Liao AH, Yu HW, Cai SR, Tien DC, Jeng SC, Chiou JF. Fast Fourier transform combined with phase leading compensator for respiratory motion compensation system. *Quant Imaging Med Surg* 2020;10(5):907-920. doi: 10.21037/qims.2020.03.19